Article

pubs.acs.org/Biomac

Changes in Glycogen Structure over Feeding Cycle Sheds New Light on Blood-Glucose Control

Mitchell A. Sullivan,[†,‡] Samuel T. N. Aroney,[‡] Shihan Li,[†,‡] Frederick J. Warren,[‡] Jin Suk Joo,[§] Ka Sin Mak,[∥] David I. Stapleton,[⊥] Kim S. Bell-Anderson,[§] and Robert G. Gilbert*[,†,‡]

[†]Tongji School of Pharmacy, Huazhong University of Science and Technology, Wuhan, Hubei 430030, China

[‡]The University of Queensland, Centre for Nutrition and Food Sciences, Queensland Alliance for Agriculture and Food Innovation, Brisbane, Queensland 4072, Australia

[§]School of Molecular Bioscience, University of Sydney, Sydney, New South Wales 2006, Australia

[∥]School of Biotechnology and Biomolecular Sciences, University of New South Wales, Kensington, New South Wales 2033, Australia

[⊥]Department of Physiology, The University of Melbourne, Parkville, Victoria 3052, Australia

Supporting Information

ABSTRACT: Liver glycogen, a highly branched polymer of glucose, is important for maintaining blood-glucose homeostasis. It was recently shown that *db*/*db* mice, a model for Type 2 diabetes, are unable to form the large composite glycogen α particles present in normal, healthy mice. In this study, the structure of healthy mouse-liver glycogen over the diurnal cycle was characterized using size exclusion chromatography and transmission electron microscopy. Glycogen was found to be formed as smaller β particles, and then only assembled into large α particles, with a broad size distribution, significantly after the time when glycogen content had reached a maximum. This pathway, missing in diabetic animals, is likely to give optimal blood-glucose control during the daily feeding cycle. Lack of this control may contribute to, or result from, diabetes. This discovery suggests novel approaches to diabetes management.

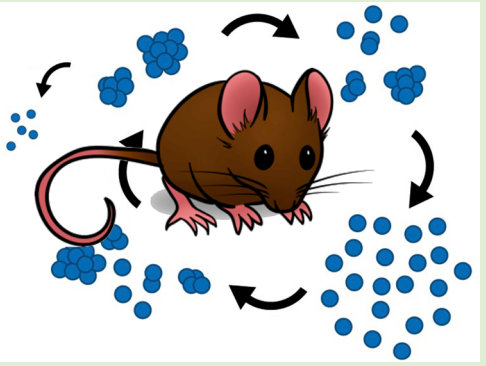

INTRODUCTION

Glycogen, a hyperbranched glucose polymer, is found in a number of organisms; in the case of animals, including humans, it is present in a variety of different tissues. Liver glycogen acts as a blood-glucose buffer, helping the body maintain blood-glucose homeostasis. Glycogen particles range from smaller β particles (~20−30 nm in diameter) to composite α particles as large as 300 nm.[1,2]

Size exclusion chromatography (SEC) has recently been used to compare the structure of nondiabetic liver glycogen with that in *db*/*db* mice, a model for type 2 diabetes.[3] The results show that the size distribution of nondiabetic liver glycogen varies, with a wide range of sizes in a given animal, but with a predominance of very large glycogen α particles in many individuals. However, liver glycogen in "diabetic" *db*/*db* mice has relatively little size variation between mice, with all glycogen consisting predominantly of β particles within a fairly narrow size distribution, plus some small α particles. This is consistent with the observation that *db*/*db* mice had fewer "heavy particles", as inferred using sucrose density centrifugation.[4] If this is a general phenomenon, then there are potential implications for elucidation of the molecular mechanisms underlying diabetes and its management in humans.

The first step in understanding why *db*/*db* mice are unable to form larger α particles is to gain a better understanding of the formation and degradation of these particles in healthy, nondiabetic mice.

Liver glycogen in mice, like many animal species,[5−8] follows a daily rhythm. This rhythm in rodents has been studied in some detail during a 12 h light/12 h dark cycle, with glycogen content peaking during the dark period and decreasing during the light (due to their nocturnal nature).[5,6,9−11] Previous results and conclusions for glycogen structural changes during synthesis and degradation have been conflicting. In 1967, Parodi reported[12] that, while glycogen content increased significantly after administering glucose to overnight-fasted mice, the glycogen size distributions (using sucrose gradient centrifugation) remained almost unchanged. However, Geddes in 1971[13] found that sucrose-density-centrifugation size distributions varied significantly with glycogen content in refed rabbits after 4 days of starvation.

Moreover, liver-glycogen contents after the refeeding of starved rats[14] and rabbits[13] were significantly higher than those of normal livers with an overproduction of low molecular weight glycogen in rabbits. Thus, a starvation/refeeding

Received: November 20, 2013
Revised: December 27, 2013
Published: December 28, 2013

method may not accurately reflect the process occurring during a normal feeding cycle.

To better understand the dynamics of liver glycogen formation, we characterized liver glycogen structure by SEC and transmission electron microscopy (TEM), from mice sacrificed at various times of the day, exploiting the natural diurnal rhythms of feeding patterns in mice.

EXPERIMENTAL SECTION

Animals. Approval for the use of animals was from the University of Sydney Animal Care and Ethics Committee. Male mice on an FVB/NJ background were bred in-house and housed in standard cages (2−6 mice/cage). Temperature was controlled at 22° ± 1 °C with a 12 h dark-light cycle (lights on at 6 am). Mice were given ad libitum access to water and standard chow (6% kcal from fat, 14.3 MJ kg^{-1}, Glen Forest Specialty Feeds WA, Australia) until age 12 weeks.

At termination, 12 week old mice were anaesthetized with sodium pentobarbitone (150 mg kg^{-1} intraperitoneal). Liver was rapidly excised, snap frozen in liquid nitrogen, and stored at −80 °C.

Glycogen Extraction. Glycogen was extracted similarly to previous studies.[15,16] Approximately 200 mg of mouse liver was homogenized in 3.2 mL of glycogen isolation buffer (50 mM Tris, pH 8, 150 mM NaCl, 2 mM EDTA, 50 mM NaF, and 5 mM sodium pyrophosphate). A total of 200 μL of this homogenate was removed for glycogen content analysis. Samples were centrifuged at 6000 *g* for 10 min at 4 °C. The supernatants were then centrifuged at 300000 *g* for 1 h at 4 °C. The pellet was then resuspended in glycogen isolation buffer and layered over a 3 mL, stepwise sucrose gradient (37.5 and 75% in glycogen isolation buffer). These samples were then centrifuged at 488300 *g* for 2 h at 4 °C. The pellet of glycogen at the bottom of the tube was resuspended in 500 μL of water. Samples were mixed with four parts absolute ethanol to precipitate glycogen. The samples were centrifuged at 4000 *g* for 10 min and the pellets were redissolved in 1 mL of deionized water and lyophilized (freeze-dried; VirTis, Benchtop K). A small amount of sample was put aside for TEM.

Size-Exclusion Chromatography. As shown previously in refs 17 and 18, mouse-liver glycogen was dissolved directly into the SEC eluent, dimethyl sulfoxide (DMSO; HPLC grade, Sigma-Aldrich) with 0.5 wt % LiBr (ReagentPlus) on a thermomixer at 80 °C for 6 h, giving complete molecular dissolution. The size separation method follows that performed previously.[17] Samples were injected into an Agilent 1100 Series SEC system (PSS, Mainz, Germany) using a GRAM preColumn, 30 and 3000 columns (PSS) in a column oven at 80 °C and a flow rate of 0.3 mL min^{-1}. This flow rate was employed to minimize shear scission of the molecules.[19] SEC weight distributions were determined by using a refractive index detector (RID; Shimadzu RID-10A, Shimadzu, Japan).

A universal calibration curve was obtained using pullulan standards (PSS), with a molar mass range of 342 to 2.35 × 10^6 Da, which were directly dissolved into the DMSO/LiBr eluent. This allowed the conversion of elution volume into hydrodynamic radius (R_h).[19] It is noted that the IUPAC definition of hydrodynamic radius[20] depends on the technique used, and thus, R_h as defined by the SEC separation parameter is a (hopefully only slightly) different quantity to that for, for example, dynamic light scattering. While there are obvious problems with this definition, it is the one that is internationally agreed upon. It could be supplanted by adding a further subscript indicating the technique in question, but to do that here, where only a single type of R_h is under discussion, would introduce an unnecessary clutter in notation. The Mark−Houwink parameters for pullulan in DMSO/LiBr (0.5 wt %) at 80 °C are $K = 2.427 \times 10^{-4}$ dL g^{-1} and $\alpha = 0.6804$ (Kramer and Kilz, PSS, private communication); this gives an R_h upper limit of accurate calibration of ∼60 nm, with the size scale above this being only semiquantitative.

Transmission Electron Microscopy. TEM images of glycogen were obtained using a similar method to that employed previously.[21] One glycogen sample from each of the mice sacrificed at 9 pm, 4 am, 12 noon, 4 pm, and after 16 h of starvation was dissolved into deionized water (∼0.5 mg mL^{-1}). This was then diluted 10-fold and applied to a glow discharged 100 mesh copper grid (ProSciTech). After 1 min, excess sample was drawn off with filter paper and 2−3 drops of 2% uranyl acetate was added to stain the sample. Excess uranyl acetate was removed using filter paper after 45 s. The preparations were then analyzed using a JEOL 1010 transmission electron microscope (JEOL, Tokyo, Japan) operating at 100 kV. The images were recorded digitally with a SIS Veleta CCD camera (Olympus, Münster, Germany) and reports and measurements were prepared using the AnalySiS image management software.

Glycogen Content Assays. The method employed, using amyloglucosidase to degrade glycogen to individual glucose units and then glucose oxidase/peroxidase (GOPOD) reagent to quantify the amount of glucose, was similar to that used elsewhere.[22] A total of 5 μL of amyloglucosidase (Megazyme), 20 μL of homogenate (from Glycogen Extraction), and 100 μL of sodium acetate buffer (pH 6) was made up to 0.5 mL with deionized water and incubated on a thermomixer at 50 °C for 30 min. A control, with everything except amyloglucosidase, was also analyzed. A 300 μL aliquot of each sample was then added to 1 mL of glucose oxidase/peroxidase reagent (GOPOD, Megazyme) and incubated for a further 30 min at 50 °C on a thermomixer. The absorbance (510 nm) of each sample was then analyzed on a UV-1700 PharmaSpec UV−vis spectrophotometer (Shimadzu). The glycogen content was then calculated based on a calibration curve (constructed by reacting D-glucose of various concentrations with the same GOPOD reagent). All samples and controls were run in duplicate with the absorbance values averaged.

RESULTS AND DISCUSSION

As shown in Figure 1, the amount of liver glycogen in the mice followed a diurnal pattern, being synthesized during the dark

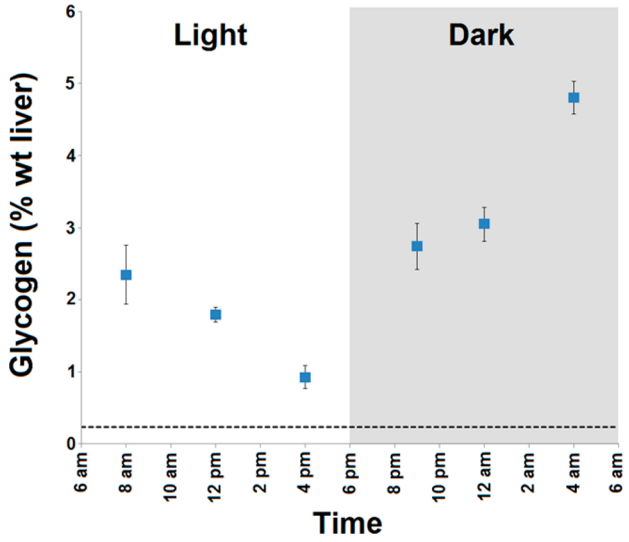

Figure 1. Liver-glycogen content of ad libitum fed wild-type mice at various stages of a day/night cycle; shading represents night/feeding period. Values shown are the mean ± SEM of 3−9 mice. The dashed line represents the mean glycogen content of 7 mice starved for 16 h.

(feeding) period and subsequently degraded during the light hours. This resembles the pattern reported in previous studies.[5,23,24] Glycogen structure was characterized at various phases of this cycle, to examine changes during glycogen synthesis, degradation, and after starvation.

SEC weight distributions of glycogen, as functions of molecular size (the hydrodynamic radius R_h) at various time points of the diurnal cycle, are given in Figure 2. The areas of the curves were normalized to unity, to give an indication of the relative structural changes. Distributions of glycogen are also

dx.doi.org/10.1021/bm401714v | Biomacromolecules 2014, 15, 660−665

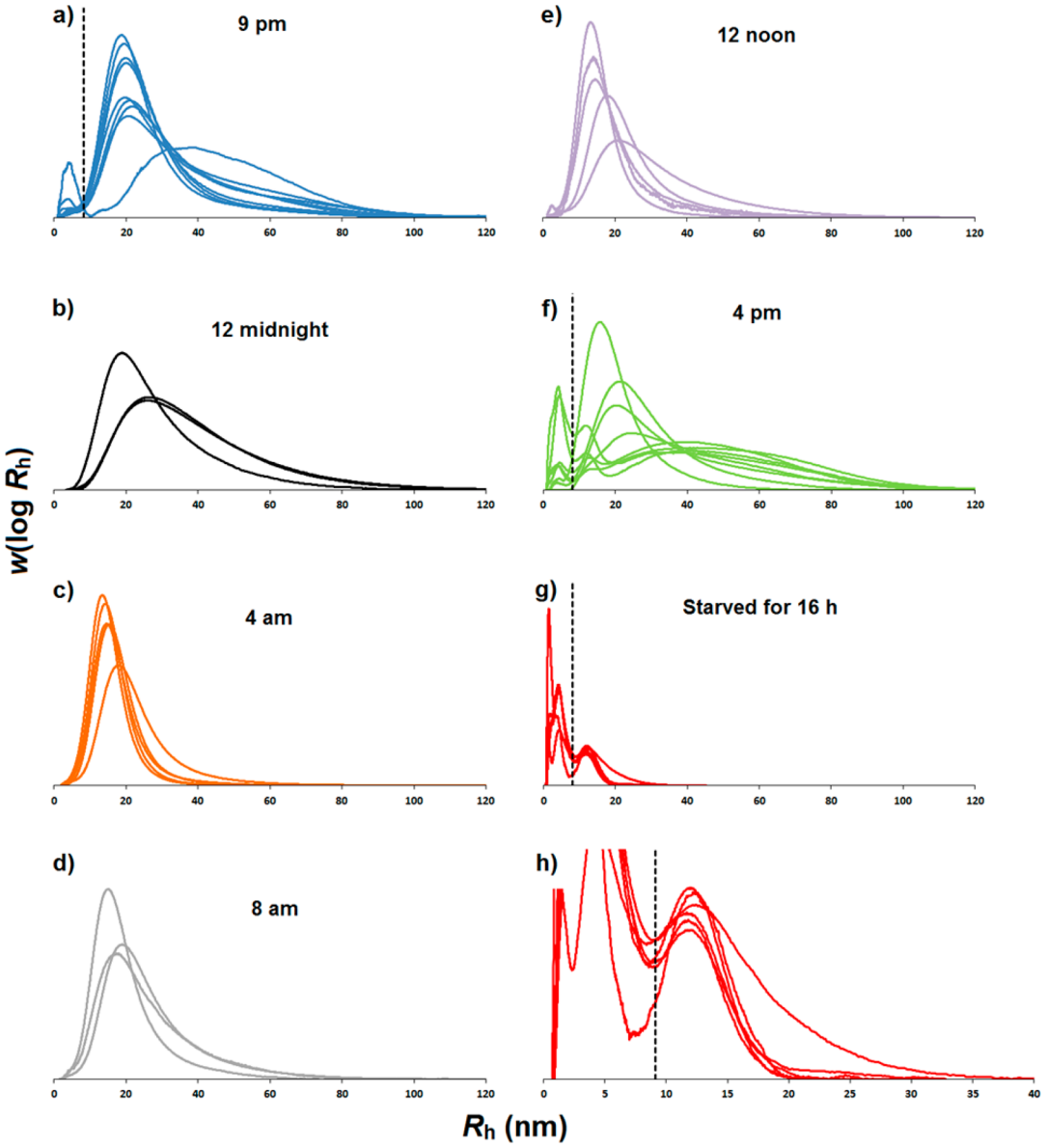

Figure 2. SEC weight distributions, $w(\log R_h)$; normalized to equal areas) as functions of molecular size (the hydrodynamic radius R_h) for wild-type mice sacrificed at various stages of the day/night cycle: 9 pm, blue (a); midnight, black (b); 4 am, orange (c); 8 am, gray (d); 12 noon, purple (e); 4 pm, green (f); after 16 h starvation, red (g); and a magnified version of (g), (h). The multiple distributions for each time point represent replicates with each distribution being from one mouse. A dashed line is added in a, f, g, and h to separate the glycogen peaks from the contamination peaks (which are much more prominent when glycogen concentrations are low) of small molecules. Note the x axis is linear in R_h, not logarithmic as normal for SEC weight distributions; the linear axis enables particular features to be distinguished for the present system. The mean values (and SEM bars) for the R_h at which the maximum occurs and the average R_h are given in the SI (Figure S1a and S1b, respectively).

normalized to their concentration in Figure 3, with the synthesis and degradation phases represented in Figure 3a and b, respectively.

Surprisingly, when glycogen reaches a maximum concentration at 4 am (Figure 1), it consists almost entirely of β particles, as seen in Figures 2c and 3a. This decrease in the average size of glycogen particles between 4 pm and 4 am is statistically significant (Figure S1 in Supporting Information). The micrographs from TEM (Figure 4b) support the suggestion that glycogen forms initially as separate β particles, which later in some way form α particles.

It cannot be confirmed whether these mice were ever going to form α particles, as approximately half of the distributions at later time points during degradation (8 am and 12 noon) also did not contain a significant population of α particles. Further studies are required to properly understand the synthesis of liver glycogen in terms of structure.

Figure 2f shows the glycogen size distributions of mice sacrificed at 4 pm, toward the end of degradation. Interestingly, large glycogen α particles still remain, with a greater proportion of the smaller molecules having been degraded. This increase in the average particle size from 12 to 4 pm is statistically significant (Figure S1 in Supporting Information). TEM was used to visualize these α particles (Figure 4d).

Where Parodi reported that the molecular weight of glycogen did not significantly change after fasting,[12] the mice were only fasted for 5 h after sacrificing the controls early in the morning, and the glycogen content decreased by ~62%. If the highest

dx.doi.org/10.1021/bm401714v | Biomacromolecules 2014, 15, 660−665

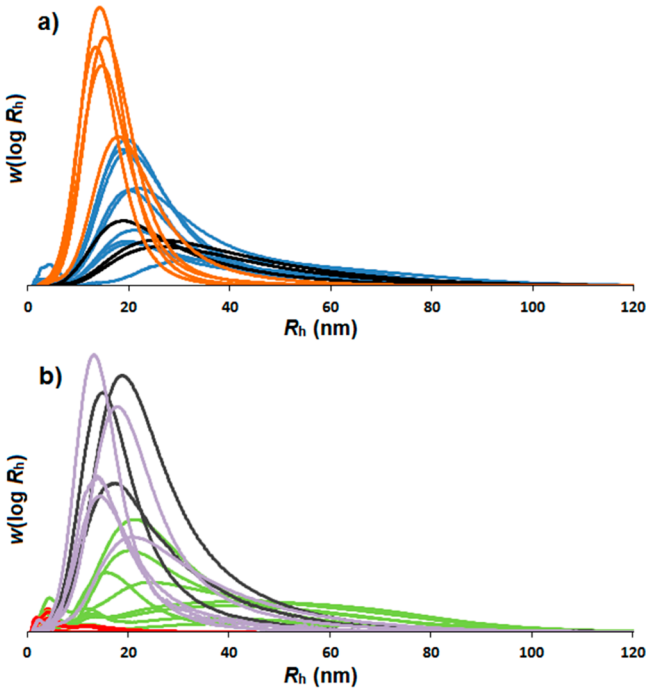

Figure 3. Same SEC weight distributions of liver glycogen from Figure 2. These are separated into the phases of glycogen synthesis (a) and degradation (b) with mice being sacrificed at 9 pm, blue (a); midnight, black (a); 4 am, orange (a); 8 am, gray (b); 12 noon, purple (b); 4 pm, green (b); after 16 h starvation, red (b). The multiple distributions represent replicates with each distribution being from one mouse. All distributions are now normalized to have an area equal to their calculated concentration.

glycogen content in the present study (~5%, see Figure 1) were to decrease by the same amount, there would be a glycogen content of ~2% (roughly that of mice sacrificed at 12 noon). It can be seen from Figure 2e that this glycogen would more likely have a distribution similar to the glycogen during the synthesis phase, but Figure 2f shows that one only has significantly different distributions at a glycogen content as low as ~1%. This suggests that if the past study had been for mice fasted for longer, the results might have been very different.

Our results agree with Geddes'[25] finding of a significant differences in sucrose-density-centrifugation distributions of liver glycogen at different times after starvation, with no large glycogen molecules remaining after 16 h of fasting (Figure 2g,h); it is noted that one can only make qualitative inferences from data obtained from sucrose-density centrifugation.

While liver glycogen reaches low levels after starvation, this glycogen can persist for up to 72 h of starvation.[26] Microscopy studies on frog hepatocytes demonstrate that starved frogs only have β particles as opposed to the α particles found in hepatocytes of fed frogs.[27] This is consistent with Figure 2g,h, where only small β particles remain during the starvation phase. These smaller β particles were visualized using TEM (Figure 4e). It is important to note that these small β particles (R_h ~12 nm) started to form during fasting (Figure 2f) when there were still large α particles present (which eventually degrade away). This, as well as the fact these molecules are narrowly distributed, suggests that they are more resistant to degradation and are not just persisting because glycogen degradation pathways are switched off.

Altogether, the size distributions of glycogen being synthesized, degraded and after starvation have revealed a number of interesting insights into glycogen metabolism, leading to the proposed "recycling" model of glycogen metabolism in terms of the tertiary structure (β and α particles) presented in Figure 5.

When glycogen reaches its maximum concentration ("Late synthesis" in Figure 5), it appears to consist almost entirely of β particles. This result, which at first is surprising, shows that α particles are formed following the formation of individual β particles.

This pathway makes evolutionary sense, with the need to rapidly synthesize large amounts of glycogen (when blood sugar is rising from the digestion of food) being aided by the higher surface area to volume ratio of the smaller β particles. Indeed it has been shown in vitro with rabbit-liver glycogen that, in the direction of synthesis, glycogen phosphorylase has a higher activity for smaller glycogen molecules.[28] Further support for this hypothesis comes from a study demonstrating a tendency for radiolabeled glucose to be incorporated more readily into lower molecular weight material.[25] Our data also suggest that α particles remaining from the previous day/night cycle appear to be degraded during glycogen synthesis (arrows 1 and 2 in Figure 5). If this were not the case, glycogen α particles that were not degraded in one diurnal cycle would continually grow during the following synthetic phase, making even larger α particles than the previous cycle. This would result in the average size of glycogen particles becoming larger from one day to the next.

During fasting, however, it is desirable to have a slower, more controlled, release of glucose back into the blood, which is aided by the transformation of many β particles into larger α particles. As stated, our results show an initial, preferential degradation of smaller molecules in the liver (arrow 4 in Figure 5), which is consistent with past studies that show glycogen phosphorylase is more associated with,[29] and has a higher in vitro activity for,[30] lower molecular weight glycogen. A radioactivity study also hinted that larger molecules may be metabolized more slowly.[13] These results and preliminary rate

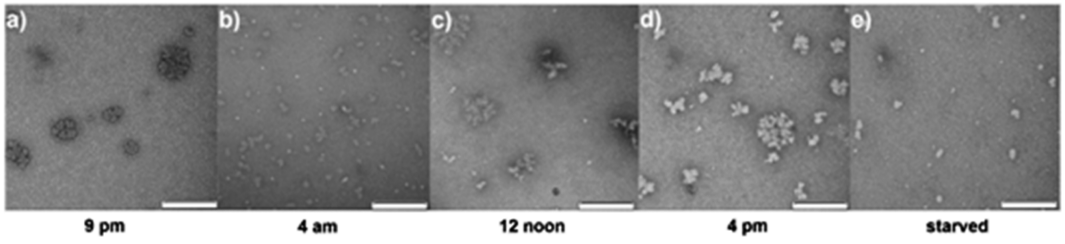

Figure 4. TEM images of liver glycogen at various stages of the day/night cycle: 9 pm (a); 4 am (b); 12 pm (c); 4 pm (d); and after 16 h of starvation (e). Scale bar represents 200 nm.

dx.doi.org/10.1021/bm401714v | Biomacromolecules 2014, 15, 660−665

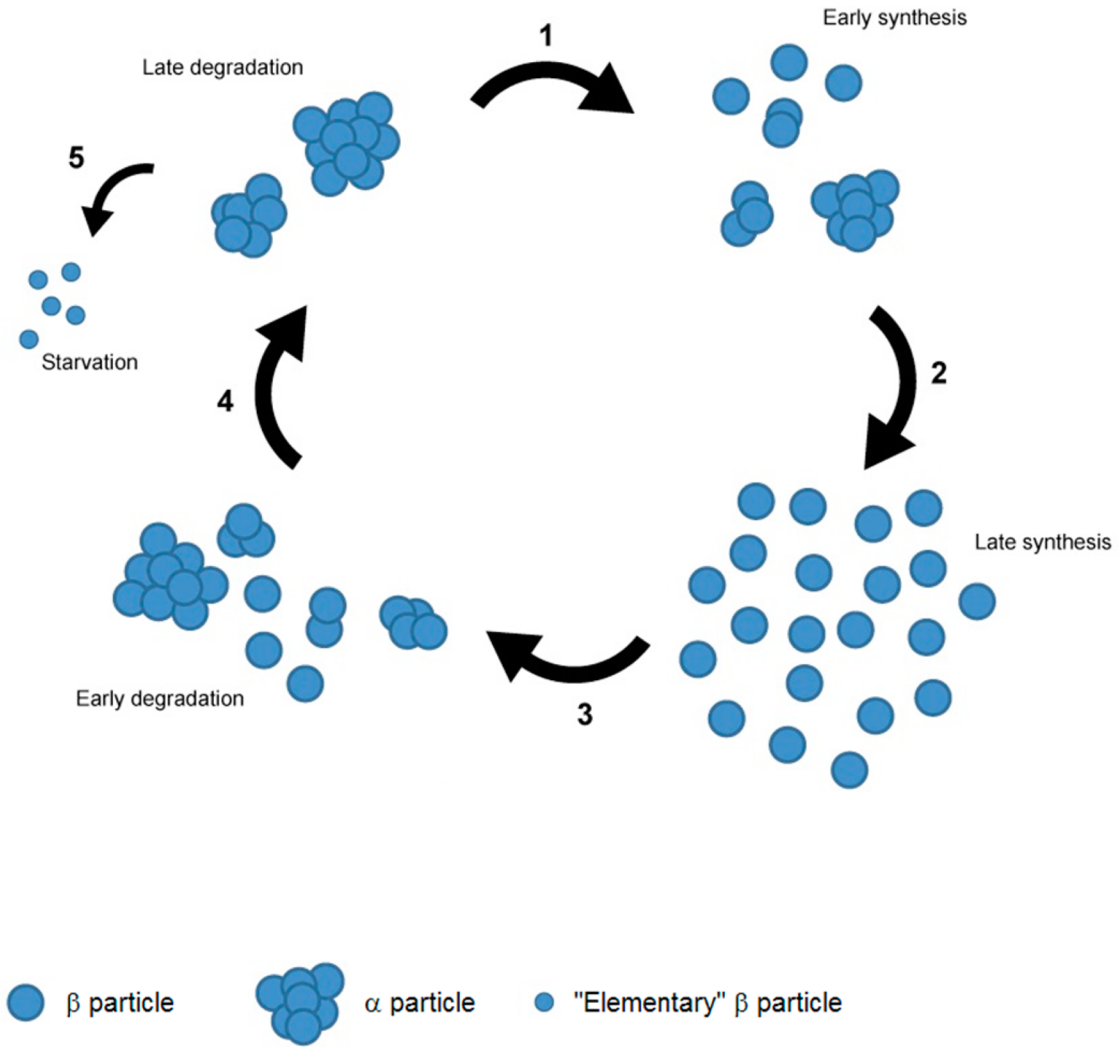

Figure 5. Proposed "recycling" model for the structural changes of glycogen over a diurnal cycle and after starvation.

data from our laboratories (showing populations of large glycogen particles degrading much slower than populations of smaller β particles; see Figure S3 in SI) support the inference that the rates of degradation per mass of glycogen of small glycogen molecules are faster than those of large molecules, consistent with the hypothesis that glycogen degradation is controlled by surface area. The observation that diabetic mice are unable to form as many large α particles as healthy mice[3] therefore suggests that these smaller molecules are more vulnerable to enzymatic degradation due to their lower ratio of surface area to volume.[3,31]

Another interesting feature of our data is the narrowly distributed small β particles that remain after starvation. An evolutionary advantage of this resistant glycogen is clear, as synthesizing a new glycogen molecule from the beginning (involving the production of more initiating protein, glycogenin) would require more energy, and be much slower, than building glycogen from this resistant "elementary" glycogen molecule. While the mechanism for the resistance of these molecules is unclear, it has been suggested that this remaining liver glycogen may be denser, impeding the access of degradative enzymes.[13,32,33] Whether this glycogen bears any relation to the proglycogen referred to in previous publications[34−36] is hard to determine due to the different glycogen-extraction methods employed; however, it has been suggested[37] that the "proglycogen" inferred in these past studies were artifacts of the extraction methods.

CONCLUSION

Size distributions of glycogen being synthesized, degraded, and after starvation have revealed a number of interesting insights into glycogen metabolism. When glycogen reaches its maximum concentration it appears to consist almost entirely of β particles. This surprising result suggests that α particles may be formed after the formation of separate β particles. A very important new discovery (consistent with past studies that suggested this may be the case) is that as glycogen degrades the larger α particles persist longer than the smaller particles and that this glycogen is degraded to a more stable molecule with an R_h of ∼12 nm. Given the lack of large α particles in diabetic animals, these findings have potential application in drug targets for diabetes management, through drugs which affect different steps in the pathway of Figure 5, a pathway whose existence was never previously suspected.

dx.doi.org/10.1021/bm401714v | *Biomacromolecules* 2014, 15, 660−665

■ ASSOCIATED CONTENT

Supporting Information

Statistical analysis of differences between the mean hydrodynamic radii at which the maximum occurs and the average hydrodynamic radii of glycogen extracted at various time points, as well as, preliminary kinetics data. This material is available free of charge via the Internet at http://pubs.acs.org.

■ AUTHOR INFORMATION

Corresponding Author

*Fax: +61 7 3365 1188. Tel.: +61 7 3365 4809. E-mail: b.gilbert@uq.edu.au.

Notes

The authors declare no competing financial interest.

■ ACKNOWLEDGMENTS

We thank Ms. Thillini Jayasinghe for assistance with the transport of tissue samples. The authors also gratefully thank Ms. Sarah Chung and Ms. Kai Wang for their technical assistance with SEC analysis. Electron microscopy was carried out in the Centre for Microscopy and Microanalysis at the University of Queensland, a node of the Australian Microscopy and Microanalysis Research Facility (AMMRF). The authors would also like to thank Professor Ling Zheng, Ms. Jiong Li, and Dr. Chuanzhou Li for their assistance with the mice used for the kinetics studies presented in the Supporting Information. We also gratefully acknowledge Ms. Thea Darnell's design skills used to create Figure 5.

■ REFERENCES

(1) Drochmans, P. *J. Ultrastruct. Res.* **1962**, *6*, 141−63.
(2) Rybicka, K. K. *Tissue Cell* **1996**, *28*, 253−265.
(3) Sullivan, M. A.; Li, J.; Li, C. Z.; Vilaplana, F.; Stapleton, D.; Gray-Weale, A. A.; Bowen, S.; Zheng, L.; Gilbert, R. G. *Biomacromolecules* **2011**, *12*, 1983−1986.
(4) Roesler, W. J.; Pugazhenthi, S.; Khandelwal, R. L. *Mol. Cell. Biochem.* **1990**, *92*, 99−106.
(5) Roesler, W. J.; Khandelwal, R. L. *Int. J. Biochem.* **1985**, *17*, 81−85.
(6) Mukerjea, R.; Robyt, J. F. *Carbohydr. Res.* **2013**, *372*, 55−59.
(7) Kim, H. J.; White, P. J. *J. Agric. Food Chem.* **2013**, *61*, 3270−3277.
(8) Cohn, C.; Joseph, D. *Proc. Soc. Exp. Biol. Med.* **1971**, *137*, 1303−1306.
(9) Halberg, F.; Albrecht, P. G.; Barnum, C. P. *Am. J. Physiol.* **1960**, *199*, 400−402.
(10) Ishikawa, K.; Shimazu, T. *Life Sci.* **1976**, *19*, 1873−1878.
(11) Philippens, K. M. H.; Vonmayersbach, H.; Scheving, L. E. *J. Nutr.* **1977**, *107*, 176−193.
(12) Parodi, A. J. *Arch. Biochem. Biophys.* **1967**, *120*, 547−&.
(13) Geddes, R.; Stratton, G. C. *Carbohydr. Res.* **1977**, *57*, 291−9.
(14) Maddaiah, V. T.; Madsen, N. B. *Can. J. Biochem.* **1968**, *46*, 521.
(15) Parker, G. J.; Koay, A.; Gilbert-Wilson, R.; Waddington, L. J.; Stapleton, D. *Biochem. Biophys. Res. Commun.* **2007**, *362*, 811−815.
(16) Ryu, J.-H.; Drain, J.; Kim, J. H.; McGee, S.; Gray-Weale, A.; Waddington, L.; Parker, G. J.; Hargreaves, M.; Yoo, S.-H.; Stapleton, D. *Int. J. Biol. Macromol.* **2009**, *45*, 478−482.
(17) Zhou, Z. K.; Cao, X. H.; Zhou, J. Y. H. *Starch-Starke* **2013**, *65*, 509−516.
(18) Sullivan, M. A.; O'Connor, M. J.; Umana, F.; Roura, E.; Jack, K.; Stapleton, D. I.; Gilbert, R. G. *Biomacromolecules* **2012**, *13*, 3805−3813.
(19) Cave, R. A.; Seabrook, S. A.; Gidley, M. J.; Gilbert, R. G. *Biomacromolecules* **2009**, *10*, 2245−53.
(20) Jones, R. G.; Kahovec, J.; Stepto, R.; Wilks, E. S.; Hess, M.; Kitayama, T.; Metanomski, W. V., *Compendium of Polymer Terminology and Nomenclature, IUPAC Recommendations 2008*; Royal Society of Chemistry: Cambridge, 2009.
(21) Ryu, J.-H.; Drain, J.; Kim, J. H.; McGee, S.; Gray-Weale, A.; Waddington, L.; Parker, G. J.; Hargreaves, M.; Yoo, S.-H.; Stapleton, D. *Int. J. Biol. Macromol.* **2009**, *45*, 478−482.
(22) Roehrig, K. L.; Allred, J. B. *Anal. Biochem.* **1974**, *58*, 414−21.
(23) Roesler, W. J.; Helgason, C.; Gulka, M.; Knandelwal, R. L. *Horm. Metab. Res.* **1985**, *17*, 572−575.
(24) Chen, C. B.; Williams, P. F.; Cooney, G. J.; Caterson, I. D. *Int. J. Obesity* **1992**, *16*, 913−921.
(25) Geddes, R. *Int. J. Biochem.* **1971**, *2*, 657−&.
(26) Cardell, R. R.; Larner, J.; Babcock, M. B. *Anat. Rec.* **1973**, *177*, 23−37.
(27) Baic, D.; Ladewski, B. G.; Frye, B. E. *J. Exp. Zool.* **1979**, *210*, 381−405.
(28) Stetten, M. R.; Stetten, D. *J. Biol. Chem.* **1958**, *232*, 489−504.
(29) Barber, A. A.; Orrell, S. A.; Bueding, E. *J. Biol. Chem.* **1967**, *242*, 4040−&.
(30) Orrell, S. A.; Bueding, E. *J. Biol. Chem.* **1964**, *239*, 4021−6.
(31) Besford, Q. A.; Sullivan, M. A.; Zheng, L.; Gilbert, R. G.; Stapleton, D.; Gray-Weale, A. *Int. J. Biol. Macromol.* **2012**, *51*, 887−91.
(32) Brammer, G. L.; Rougvie, M. A.; French, D. *Carbohydr. Res.* **1972**, *24*, 343−354.
(33) Geddes, R. *Carbohydr. Res.* **1968**, *7*, 493−497.
(34) Alonso, M. D.; Lomako, J.; Lomako, W. M.; Whelan, W. J. *FASEB J.* **1995**, *9*, 1126−1137.
(35) Lomako, J.; Lomako, W. M.; Whelan, W. J. *FEBS Lett.* **1991**, *279*, 223−228.
(36) Lomako, J.; Lomako, W. M.; Whelan, W. J. *Eur. J. Biochem.* **1995**, *234*, 343−349.
(37) James, A. P.; Bames, P. D.; Palmer, T. N.; Fournier, P. A. *Metab., Clin. Exp.* **2008**, *57*, 535−543.